
*Carnegie Observatories Astrophysics Series, Vol. 5:
RR Lyrae Stars, Metal-Poor Stars, and the Galaxy
ed. A. McWilliam (Pasadena: Carnegie Observatories)*

RR Lyrae Variables in M31 and M33

ATA SARAJEDINI

*Department of Astronomy, University of Florida, 211 Bryant Space Science Center, Gainesville, FL
32611, USA*

Abstract

The properties of RR Lyrae variables make them excellent probes of the formation and evolution of a stellar population. The mere presence of such stars necessitates an age greater than ~ 10 Gyr while their periods and amplitudes can be used to estimate the metal abundance of the cluster or galaxy in which they reside. These and other features of RR Lyraes have been used to study the properties of M31 and M33. Though these studies are generally in their infancy, we have established that M31 and M33 do indeed harbor RR Lyraes in their halos and probably also in their disks suggesting that these two components formed early in the history of M31 and M33. The mean metallicities of the halo RR Lyraes in these galaxies are consistent with those of other halo stellar population tracers such as the dwarf spheroidal satellites of M31 and the halo globular clusters in M33. Little is known about the spatial distribution of the RR Lyraes, especially in M33. This will require wide-field time-series studies with sufficient photometric depth to allow both the identification of RR Lyraes and robust period determination.

1. Introduction

The class of pulsating stars known as RR Lyrae variables are located at the intersection of the instability strip and the horizontal branch in the Hertzsprung Russell Diagram. Their utility has been widely documented in the literature. As such, they can be referred to as the “swiss army knife” of astronomy as graphically illustrated in Fig. 1.

Because of their low masses ($\sim 0.7 M_{\odot}$, Smith 1995), the mere presence of RR Lyrae stars in a stellar population suggests an old age ($\gtrsim 10$ Gyr) for the system. As such, one does not need to obtain deep photometry beyond the old main sequence turnoff in

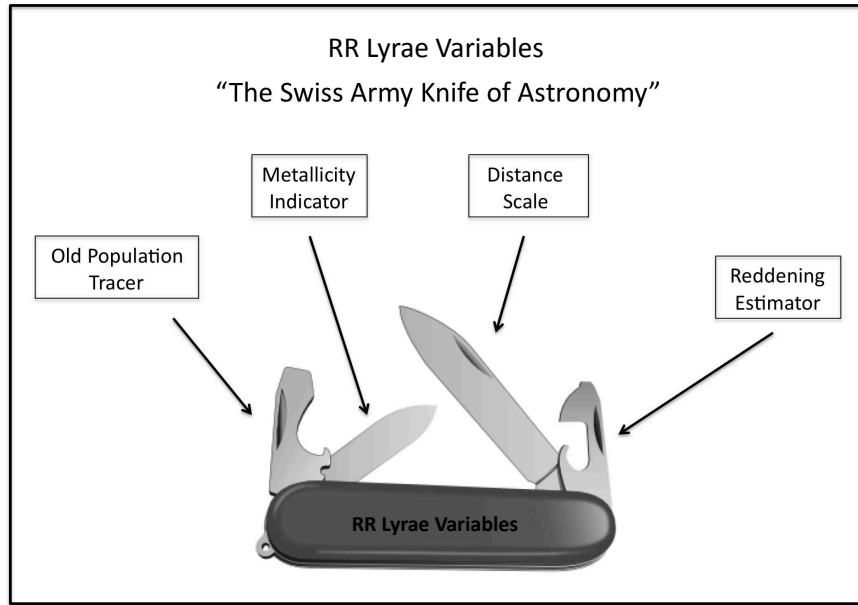


Figure 1.— Graphic illustrating the multiple uses of RR Lyrae variables in astronomy. They are well known as distance indicators, and, in addition, their mere presence necessitates the existence of a stellar population with an age greater than ~ 10 Gyr. Their periods and amplitudes are useful for measuring the metal abundance of the star cluster or galaxy in which they reside. Furthermore, their minimum light colors can be used to measure the line-of-sight reddening.

order to establish the presence of an old population. Generally speaking, *identifying* RR Lyrae variables does not require a substantial investment of telescope time.

There are three principal types of RR Lyrae variables; those pulsating in the fundamental mode exhibit sawtooth-like light curves and are referred to as ab-type or RR0 variables. The first overtone pulsators generally show sine-curve shaped light curves, have smaller periods and typically lower amplitudes than the ab-types, and are referred to as c-type or RR1 variables. Lastly, RR Lyraes that pulsate in both the fundamental and first overtone modes (i.e. double mode pulsators) carry the d-type moniker.

The periods of the ab-type RR Lyrae stars (P_{ab}) are related to their metallicities. Using data on field RR Lyraes from Layden (2005, private communication), Sarajedini et al. (2006) found

$$[Fe/H] = -3.43 - 7.82 \text{ Log } P_{ab}. \quad (1)$$

The dispersion in this relation (rms = 0.45 dex) is significant making the determination of individual stellar metallicities unreliable, but the relation is useful for estimating the mean abundance of a population of RR Lyraes. There is a more precise relation given by Alcock et al. (2000) that requires knowledge of the period *and* amplitude $[A(V)]$.

They found

$$[Fe/H] = -8.85[Log P_{ab} - 0.15A(V)] - 2.60. \quad (2)$$

With this relation, the error per star is reduced to ~ 0.31 dex and the precision of the resulting abundance distribution is narrower (Sarajedini et al. 2009).

Once the metallicities of the RR Lyraes are determined, their absolute magnitudes can be calculated. The published equations typically take the form of a linear relation between $[Fe/H]$ and $M_V(RR)$. A number of different slopes and zero-points have been derived for this equation, but there seems to be convergence on slope values of ~ 0.20 and zero-points of ~ 0.90 (Chaboyer 1999, Gratton et al. 2003, 2004; Dotter et al. 2010).

The work of Bono et al. (2007) has combined the process of metallicity and distance determination together into one coherent technique. They describe a process that uses the periods of the ab-type RR Lyraes along with their amplitudes to calculate absolute magnitudes, which are then input into a relation between $M_V(RR)$ and $[Fe/H]$ in order to determine the metal abundance. In applying this method to their observations of M31 RR Lyraes, Jeffrey et al. (2011) claim that the Bono et al. (2007) method for deriving metallicities from period and amplitude data is superior to those of Alcock et al. (2000) and Sarajedini et al. (2006).

Moving on to the reddening of the RR Lyraes, the minimum light colors of ab-type RR Lyraes are largely independent of their other properties as shown by Guldenschuh et al. (2005) and Kunder et al. (2010). This is based on a concept originally developed by Sturch (1966). As a result, if the minimum light colors are well-determined, they can be compared with $(V - I)_{o,min} = 0.58 \pm 0.02$ and $(V - R)_{o,min} = 0.28 \pm 0.02^1$ in order to measure the line-of-sight reddening for each star.

Thus far, we have presented evidence for how RR Lyrae variables can be powerful probes of the systems in which they reside - star clusters or among the field populations of galaxies. It is for this reason that studying them in the Local Group spiral galaxies M31 and M33 provides valuable insights into the properties of these systems. Ultimately, we would like to know how large spiral galaxies like M31 and ‘dwarf spirals’ like M33 fit into the process of galaxy formation in a Universe dominated by cold dark matter (CDM) with a cosmological constant Λ (Navarro, Frenk, & White 1997). Comprehensive knowledge of the most ancient stars in these systems will shed light on this question. In the remainder of this contribution, we will describe how RR Lyrae stars have been used for this purpose.

2. RR Lyraes in M31

The field RR Lyrae population of M31 was first systematically studied by Pritchett & van den Bergh (1987). They used the Canada-France-Hawaii 3.6m telescope to observe

¹ Depending on how the minimum light color is measured, this value could also be $(V - R)_{o,min} = 0.27 \pm 0.02$. See Kunder et al. (2010) for details.

a field at a distance of 9 kpc from the center of M31 along the minor axis partially overlapping the field observed by the seminal work of Mould & Kristian (1986). Pritchett & van den Bergh (1987) identified 30 RR Lyrae candidates and were able to estimate periods for 28 of them. These ab-type variables have a mean period of $\langle P_{ab} \rangle = 0.548$ days. The photometric errors in their data prevented them from identifying the lower-amplitude c-type RR Lyraes.

Dolphin et al. (2004) observed the same field as Pritchett & van den Bergh (1987) using the WIYN 3.5m on Kitt Peak. They found 24 RR Lyrae stars with a completeness fraction of 24%, suggesting that their ~ 100 square arcmin field could contain ~ 100 RR Lyraes resulting in a density of about one RR Lyrae per square arcmin. This is much less than the value of ~ 17 per square arcmin found by Pritchett & van den Bergh (1987). They also noted that the mean metallicity of the M31 RR Lyraes seemed to be significantly lower than that of the M31 halo. The work of Durrell et al. (2001) had reported a peak value of $[M/H] \sim -0.8$ for the M31 halo, and Dolphin et al. (2004) were not able to reconcile this abundance value with the distance implied by the mean magnitude of their RR Lyrae sample.

The most definitive work on the RR Lyraes of M31 was published by Brown et al. (2004) and made use of ~ 84 hours of imaging time (250 exposures over 41 days) with the Wide Field Channel of the Advanced Camera for Surveys (ACS/WFC) onboard HST. Their field was located along the minor axis of M31 approximately 11 kpc from its center. Their analysis revealed a complete sample of RR Lyrae stars consisting of 29 ab-type variables and 25 c-type. Using equation (2) above, the periods and amplitudes of these stars suggest a mean metallicity of $[Fe/H] \sim -1.7$ for the old population in the Andromeda halo. This is qualitatively consistent with the assertions of Dolphin et al. (2004) regarding the metal abundance of the M31 halo - that it is lower than the value suggested by the work of Durrell et al. (2001). As we discuss below, more recent work has shown that the M31 bulge dominates the spheroid inside ~ 30 kpc while the halo dominates from ~ 30 to ~ 165 kpc (Guhathakurta et al. 2005; Irwin et al. 2005) and has a metallicity that is comparable to that of the Milky Way halo (Kalirai et al. 2006; Koch et al. 2008).

The paper by Jeffrey et al. (2011), which is the most recent contribution in this area, is a continuation of the Brown et al. (2004) work and presents high quality light curves for RR Lyraes in 5 additional fields around M31. These include a halo field at 21 kpc, and two halo fields at 35 kpc. In addition, there is a field coincident with one of the streams in the vicinity of M31 and one that covers a disk region about 26 kpc from the center along the major axis of the galaxy. Figure 2 presents the radial density profile of M31 RR Lyraes from the studies mentioned thus far. These are compared with the surface brightness profile illustrated in Fig. 4b of Pritchett & van den Bergh (1994). The latter has been normalized to match the average of the inner two RR Lyrae points. Neglecting the point based on the work of Dolphin et al. (2004), which is an extrapolation based on a completeness correction applied to their sample, it would appear that the stream and disk fields in M31 exhibit an excess of RR Lyraes above that

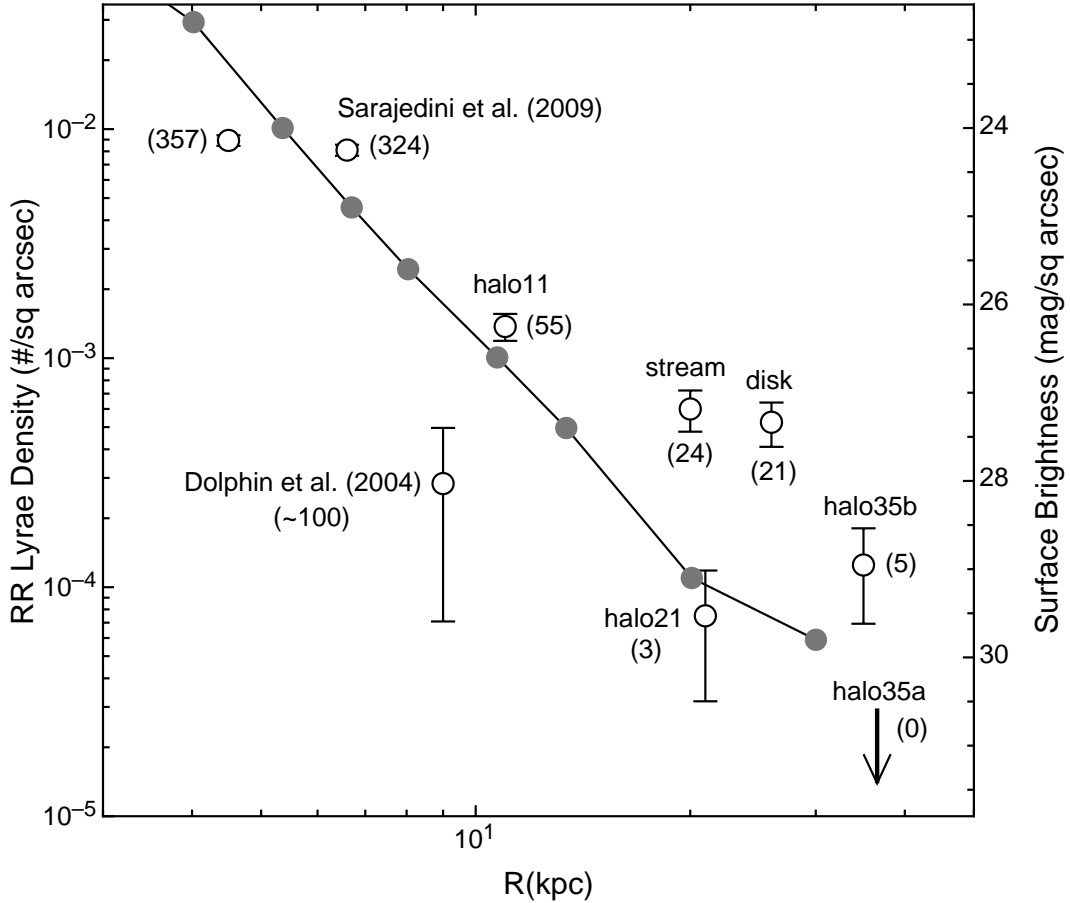


Figure 2.— The open circles represent the surface density of RR Lyrae variables identified in M31 with each point labeled based on its source. Those designated halo11, stream, disk, halo21, and halo35b are taken from the work of Jeffrey et al. (2011). Note that the Dolphin et al. (2004) value, which is based on WIYN 3.5m telescope MiniMosaic observations, represents an extrapolation based on their estimate of the incompleteness of their sample. The remaining points are all taken from HST/ACS studies. The values in parenthesis indicate the raw number of RR Lyraes in each field. The solid points connected by line segments show the surface brightness profile of M31 taken from Fig. 4b of Pritchett & van den Bergh (1994) scaled to match the average of the inner two RR Lyrae density points. Neglecting the point based on the work of Dolphin et al. (2004), it would appear that the stream and disk fields exhibit an excess of RR Lyraes above that of the M31 halo.

of the M31 halo. The surface brightness profile of the halo predicts the presence of ~ 4 halo RR Lyraes in the stream field and ~ 3 such stars in the disk field leaving ~ 20 and ~ 18 RR Lyraes in the stream and disk, respectively. If this finding withstands further scrutiny, it suggests that the oldest stars in the M31 disk, halo, and stream all have very similar ages and metallicities. Jeffrey et al. (2011) also performed a comparison of the three methods described in Sec. 1 to estimate the mean metallicity of an RR Lyrae population. They conclude that the three methods are roughly consistent with each other in terms of the derived mean metallicity of the RR Lyrae population.

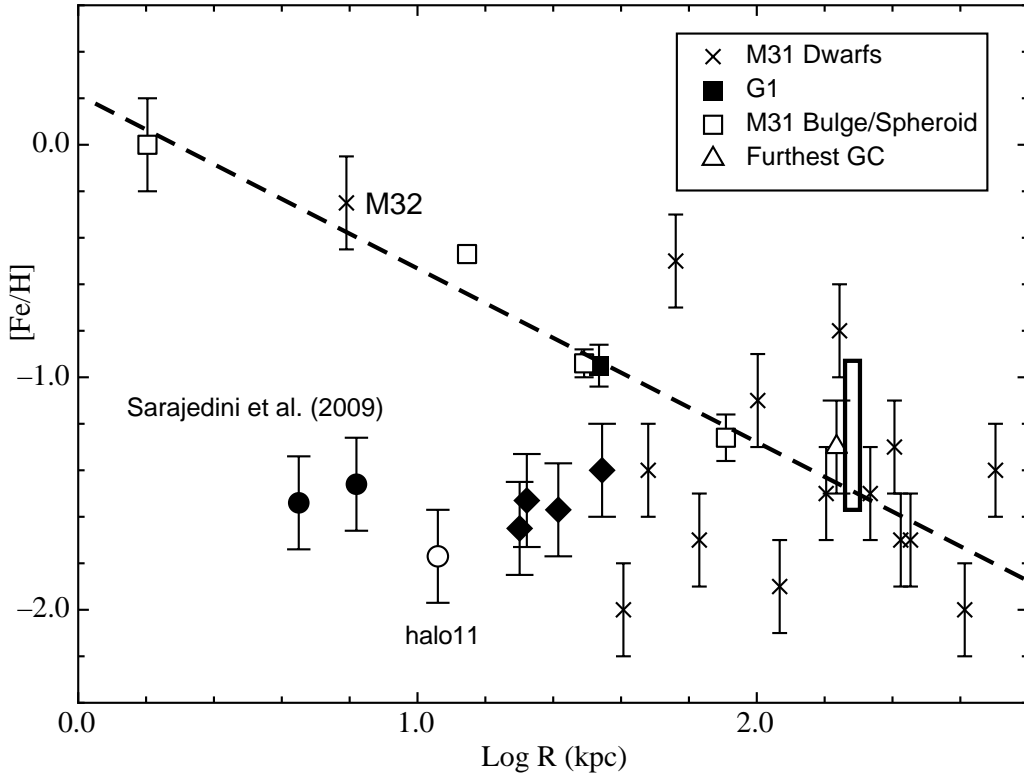


Figure 3.— A plot of the variation of metal abundance with projected distance from the center of M31. The inner most open square represents the bulge abundance measured by Sarajedini & Jablonka (2006). The remaining open squares are the bulge/halo points from the work of Kalirai et al. (2006). The dashed line is the least squares fit to these data with a slope of -0.75 ± 0.11 . The crosses represent the dwarf galaxies surrounding M31 from the work of Grebel et al. (2003) and Koch & Grebel (2006) whereas the abundance of M32 is taken from Grillmair et al. (1996). The filled square is the well-known massive globular cluster G1 studied by Meylan et al. (2001). The open triangle is the furthest known globular cluster in M31 discovered by Martin et al. (2006). The points from Sarajedini et al. (2009, filled circles) and Brown et al. (2004, open circle) are also plotted. The diamonds are the fields observed by Jeffrey et al. (2011) and designated halo21, stream, disk, and halo35b. Unless otherwise noted, an error of 0.2 dex is adopted for each point derived from the RR Lyraes. For completeness, the boxed region shows the location of the halo globular clusters in M33 from the work of Sarajedini et al. (2000). All of these points have been scaled to an M31 distance of $(m - M)_0 = 24.43$.

Sandwiched between the Brown et al. (2004) paper and its successor, the work of Jeffrey et al. 2011, is the HST/ACS study of Sarajedini et al. (2009), which is also focused on the RR Lyrae population of M31. A total of 681 RR Lyraes (555 ab-type and 126 c-type) were identified in two fields located at ~ 4 kpc and ~ 6 kpc from the center of M31. A mean metal abundance of $[Fe/H] \sim -1.5$ was determined using equation (2) above. In addition, as the Bailey diagrams shown in Fig. 10 of Sarajedini et al. (2009) and Fig. 12 of Jeffrey et al. (2011) illustrate, the RR Lyrae stars in M31 are largely consistent with the those in Oosterhoff (1939) type I Galactic globular clusters.

Seeking to place the mean metallicity of its RR Lyraes within the broader context

of the radial metallicity gradient in M31 and its environs, Sarajedini et al. (2009) constructed the plot shown in Fig. 3. The inner-most point in Fig. 3 is the bulge metallicity from the work of Sarajedini & Jablonka (2005), while the remaining open squares are the bulge/halo points from the work of Kalirai et al. (2006) as shown in their Table 3. The dashed line is the least squares fit to the open squares. The other points represent the dwarf spheroidal companions to M31 (crosses, Grebel et al. 2003; Koch & Grebel 2006), the globular cluster G1 (filled square, Meylan et al. 2001), and the furthest globular cluster in M31 (open triangle, Martin et al. 2006). Note that we have adopted the mean metallicity of M32 from the work of Grillmair et al. (1996). The metallicities for the RR Lyraes in the two fields observed by Sarajedini et al. (2009) are shown by the filled circles while the open circle represents the RR Lyraes in the halo11 field of Brown et al. (2004) field. The filled diamonds are the halo21, stream, disk, and halo35b fields in order of increasing galactocentric distance from Jeffery et al. (2011). For completeness, the elongated rectangle represents the locations of the halo globular clusters in M33 from Sarajedini et al. (2000). All of these values are based on a distance of $(m - M)_o = 24.43$ (770 kpc) for M31. In cases where an error in the metallicity is not available, we have adopted a value of ± 0.2 dex.

We see in Fig. 3 a clear representation of the notion that the halo population in M31 does not begin to dominate until a galactocentric distance of ~ 30 kpc, as suggested by a number of authors (Guhathakurta et al. 2005; Irwin et al. 2005; Kalirai et al. 2006; Koch et al. 2007). At this location, we see a transition region between the globular cluster G1 which is consistent with the inner-spheroid metallicity gradient (dashed line) and the dwarf spheroidal galaxies which show no relation between abundance and galactocentric distance. In this sense, it would appear that the RR Lyrae populations follow the trend outlined by the stellar populations outside of ~ 30 kpc. This indicates that all of the RR Lyraes, with the likely exception of those in the disk and stream fields, are probably members of the M31 halo rather than its bulge suggesting that the halo can be studied as close as 4 kpc from the center of M31 by focusing on the RR Lyraes.

3. RR Lyraes in M33

The history of RR Lyrae studies in M33 is relatively short as compared with M31. The earliest study is that of Pritchett (1988), who presented preliminary results for a handful of such stars. No data or light curves were shown, but Pritchett (1988) did estimate a distance of $(m - M)_0 = 24.45 \pm 0.2$ for M33 based on the RR Lyrae variables. This value is somewhat smaller than the average of several different determinations from Galleti et al. (2004) of $(m - M)_0 = 24.69 \pm 0.11$.

The first study to unequivocally identify and characterize RR Lyraes in M33 was that of Sarajedini et al. (2006). They used time-series observations of two fields in M33 taken with ACS/WFC onboard HST. The observations consisted of 8 epochs

in the F606W ($\sim V$) filter and 16 epochs in the F814W ($\sim I$) filter. The data were analyzed using the light curve-template-fitting software developed by Andrew Layden and described in Layden & Sarajedini (2000, see also Mancone & Sarajedini 2008). Based on these data, 64 ab-type RR Lyraes were identified. However, very few c-type variables were uncovered because of their generally lower amplitude.

The period distribution of the ab-type variables showed two peaks - one at longer periods which resembles the metal-poor RR Lyraes in M3 and M31 (Brown et al. 2004) and one at shorter periods which could be from metal-rich RR Lyraes in M33's disk. The presence of the latter population is somewhat uncertain given the recent work of Pritzl et al. (private communication). Sarajedini et al. (2006) found the mean metallicity of the metal-poor RR Lyraes to be consistent with that of halo globular clusters in M33 which have $\langle [\text{Fe}/\text{H}] \rangle = -1.27 \pm 0.11$ (Sarajedini et al. 2000).

Figure 12 of Sarajedini et al. (2006) shows that the M33 RR Lyraes are in their expected location in the color-magnitude diagram (CMD); in addition, their colors exhibit a dispersion that is consistent with being significantly affected by differential reddening. This suggests that some of the RR Lyraes are on the near side of M33 while others are in the disk and/or on the far side of the galaxy. One way to further investigate this possibility is to examine the distribution of RR Lyrae reddenings using the intrinsic minimum light color of the ab-types as mentioned in Sec. 1. This analysis was performed by Sarajedini et al. (2006) and shows that the RR Lyraes span the range from $E(V-I) < 0.1$ up to $E(V-I) \sim 0.7$. Given that the line-of-sight reddening to M33 is $E(V-I) \sim 0.1$, this suggests that RR Lyraes exist in the disk of M33 and in its halo (on the near and far side). We return to this point later as we discuss the most recent results on RR Lyraes in M33.

The primary result from the work of Sarajedini et al. (2006) was that M33 does indeed contain RR Lyrae variables in its halo. This suggests that the halo of M33 contains some fraction of stars with ages older than ~ 10 Gyr. In this regard, the halos of M33, M31, and the Milky Way are similar. It seems that they started forming stars at about the same time.

Building upon the work of Sarajedini et al. (2006), Yang et al. (2010) present an analysis of new HST/ACS/WFC imaging that is part of program GO-10190. The primary aim of this program is to study the star formation of the disk of M33 (Williams et al. 2009). As such, fields were obtained at four different disk locations roughly equally spaced along the major axis of M33. Figure 1 of San Roman et al. (2009) shows the locations of the disk fields. Here we focus on the properties of the RR Lyraes in the second closest field to the center of the M33, which we designate DISK2.

The observations are composed of 16 epochs in the F606W filter and 22 in the F814W filter spanning a time window of ~ 3 days. Template-fitting analysis suggests the presence of 86 RR Lyraes in this field - 65 ab-type, 18 c-type, and 3 d-type variables. The upper panel of Figure 4 shows the CMD of DISK2 along with the locations of the RR Lyraes. The lower panel of Fig. 4 displays the distribution in color of the ab-type RR Lyraes revealing the presence of two peaks - a primary peak at $(V-I) \sim 0.5$ and

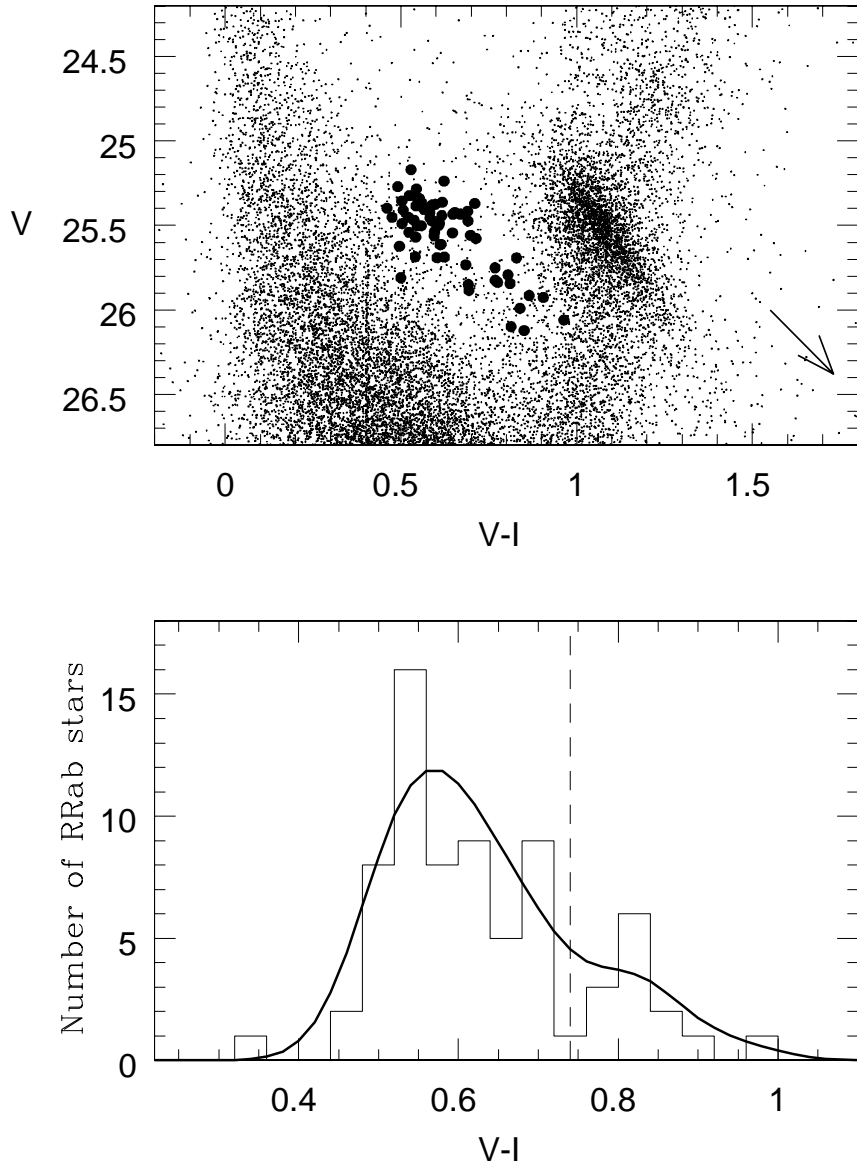


Figure 4.— The upper panel shows the color magnitude diagram of the DISK2 field from the work of Yang et al. (2010) along with the RR Lyraes identified in this field (filled circles). The brightest two or three stars are likely to be anomalous cepheids. The arrow shows the reddening vector in the CMD. The lower panel illustrates the color histogram for the RR Lyrae variables, which appears to show a bimodal distribution with a primary peak at $(V-I) \sim 0.5$ and a secondary one at $(V-I) \sim 0.8$ with a minimum around $(V-I) = 0.74$ (dashed line).

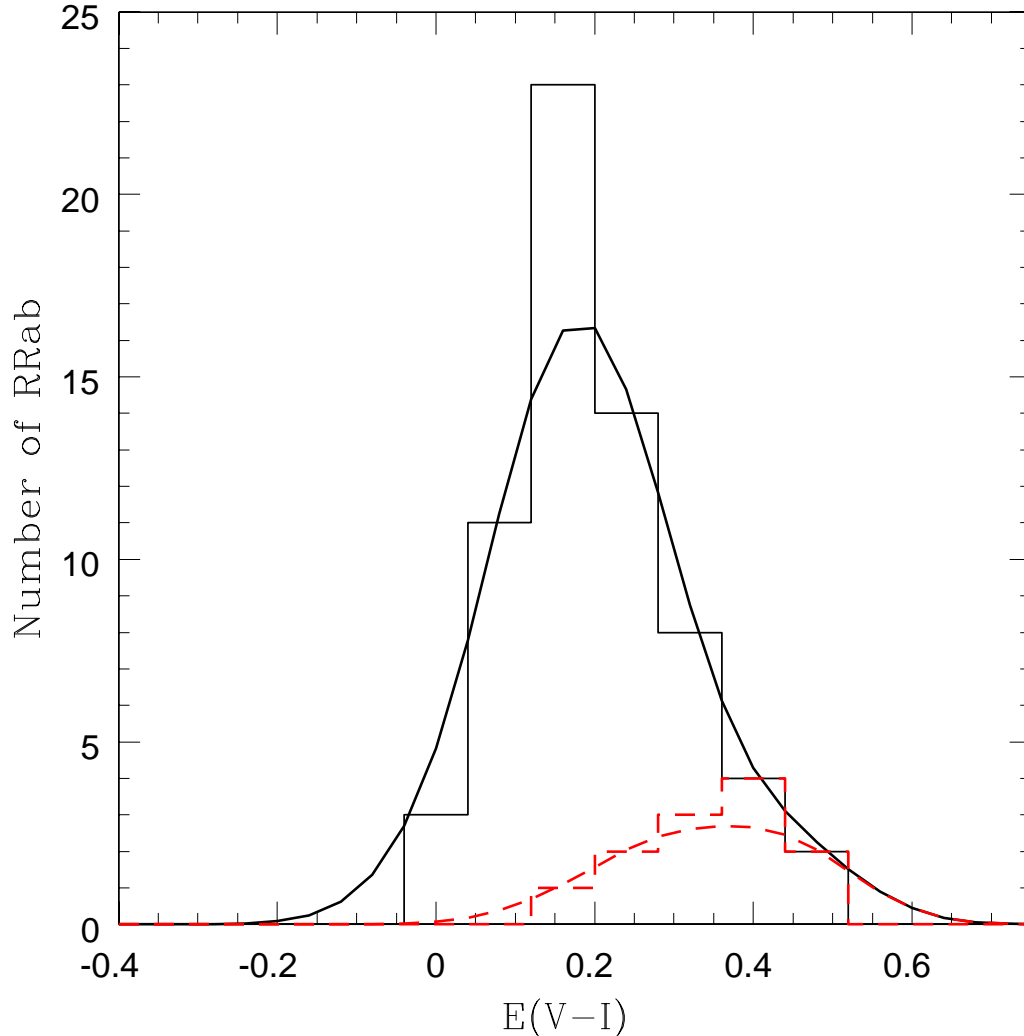


Figure 5.— The solid line is the distribution of reddenings for ab-type RR Lyrae identified in M33 from the study of Yang et al. (2010). The dashed line is the reddening distribution of RR Lyrae with $(V-I) > 0.74$ (dashed line in Fig. 4) showing that these stars are red because of reddening in the disk of M33.

a secondary one at $(V-I) \sim 0.8$. We would like to know if this bimodality is due to reddening internal to M33. As such, we determine the reddening of each RR Lyrae using Sturch’s method as described in Sec. 1 and then examine the distribution of reddenings to see if the fainter/redder RR Lyrae, those with $(V-I) > 0.74$, do indeed suffer from higher reddening. Figure 5 illustrates this effect. The solid histogram represents all ab-type RR Lyrae while the dotted histogram shows only those with $(V-I) > 0.74$ (dashed line in the bottom panel of Fig. 4). Our hypothesis seems to be correct - that the fainter/redder RR Lyrae are being affected by extinction internal

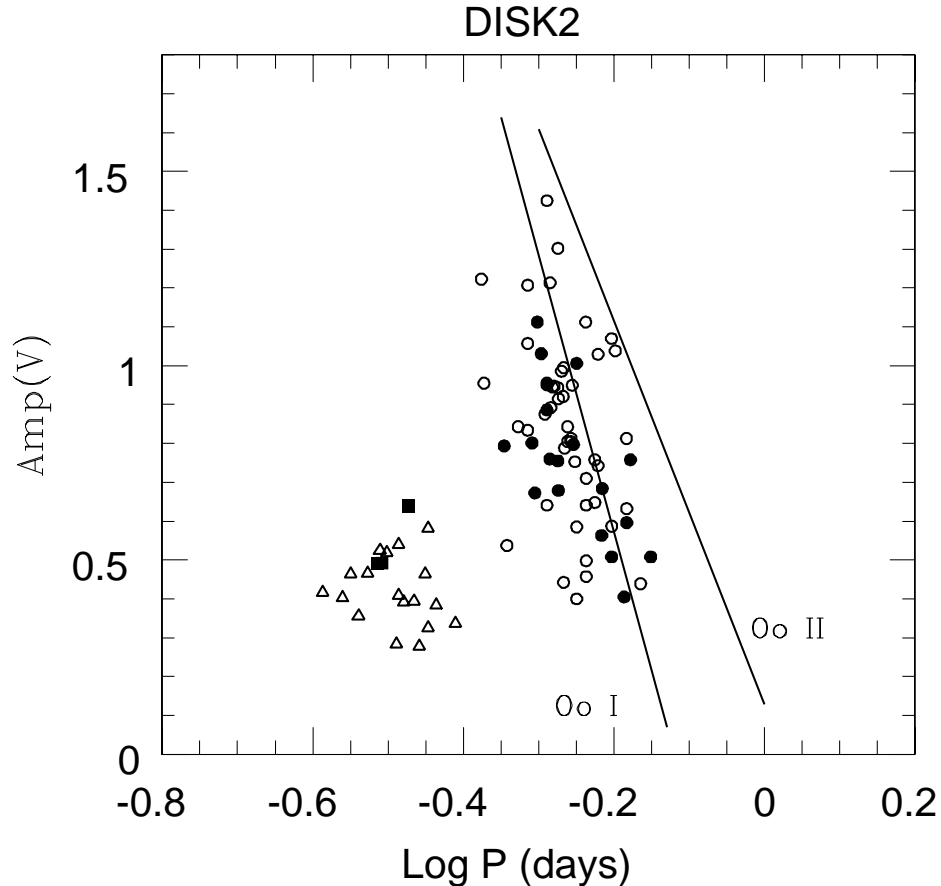


Figure 6.— This shows the Bailey Diagram for all RR Lyraes in the M33 DISK2 field. The open circles are the ab-type variables while the open triangles are the c-types. The few candidate d-type RR Lyraes are identified with filled squares. The solid lines are the locations of the Oosterhoff type I and Oosterhoff type II Galactic globular clusters from the work of Clement & Rowe (2000). The filled circles are the ab-type RR Lyraes with $(V-I) > 0.74$ from Fig. 4; these are likely to be located on the far side of M33’s disk. See text for discussion.

to M33. This suggests that the variables near $(V-I) \sim 0.5$ are on the near side of M33 while those with $(V-I) \sim 0.8$ are in the disk or on the far side.

We now seek to compare the properties of the low reddening and high reddening RR Lyraes. In particular, how do they compare in the Bailey Diagram? This is shown in Fig. 6 where we plot the periods and amplitudes of the DISK2 RR Lyraes (open circles - ab-types, open triangles - c-types; filled squares - d-types; filled circles - higher reddening ab-types). These are compared with the Oosterhoff I and II loci from Clement & Rowe (2000). We see that the ab-type RR Lyraes in M33 (both the low reddening and higher reddening samples) are consistent with those in Oosterhoff I Galactic globular clusters. This suggests that the mean metallicities of these samples are indistinguishable from each other. This reinforces the assertion that the low reddening RR Lyraes as well as most of those that suffer from higher reddening are likely to be in

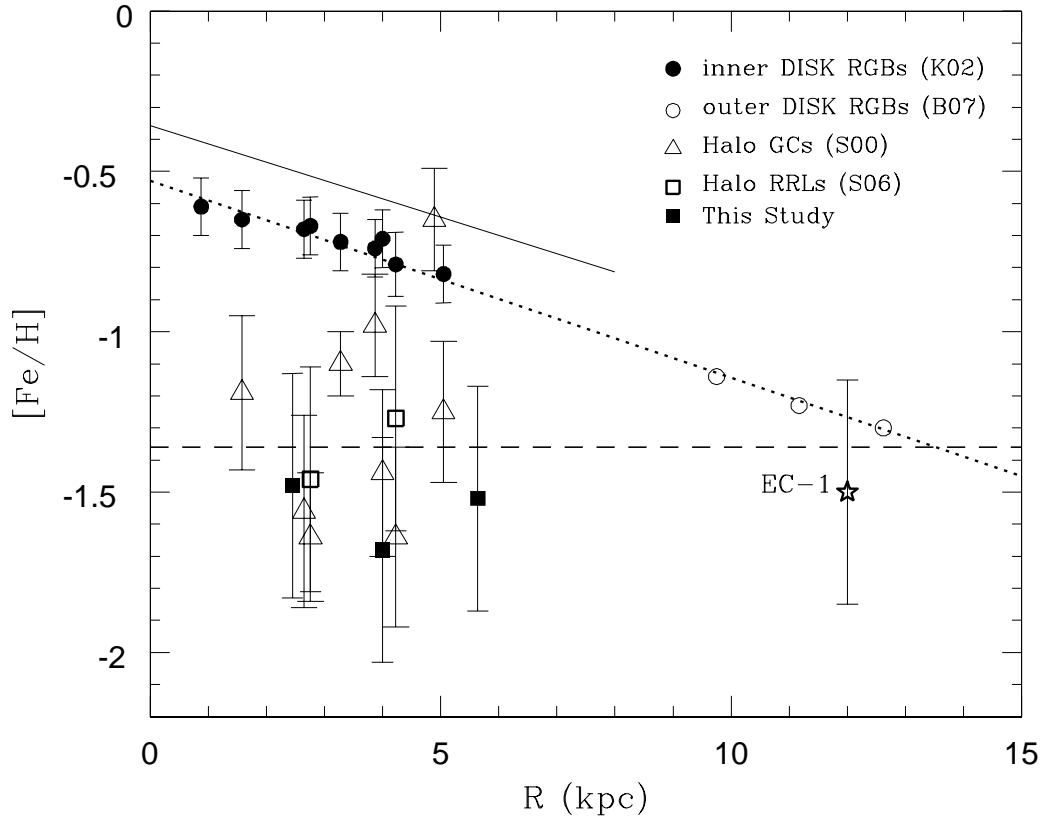


Figure 7.— The metallicity of the M33 stellar populations as a function of deprojected radial distance from the galactic center taken from Yang et al. (2010). The dotted line is a least-squares fit to the radial trend of the M33 disk red giant branch stars from Kim et al. (2002, filled circles) and also happens to coincide with the outer disk points from Barker et al. (2007, open circles). The solid line shows the metallicity trend of the M33 planetary nebulae (PNe) from Magrini et al. (2010). The dashed line represents the mean metallicity ($[Fe/H] = 1.36$) of the M33 halo stellar populations in this plot (globular cluster - open triangles, RR Lyraes - squares). The open star represents EC-1, which is the furthest known star cluster from the center of M33 (Stonkute et al. 2008). Note that “This Study” refers to the work of Yang et al. (2010) from which this figure was taken.

the halo of M33.

Similar to our analysis in M31, it is possible to examine the radial metallicity gradient in M33. Figure 7 is taken from the work of Yang et al. (2010) and shows a number of stellar populations that trace the disk and halo of M33. Figure 7 shows the inner disk fields of Kim et al. (2002, solid circles) and the outer disk fields of Barker et al. (2007, open circles) both of which are based on red giant branch samples. The dotted line is the least-squares fit to the inner disk points from Kim et al. (2002), which also reproduces the location of the outer disk points from Barker et al. (2007). The solid line in Figure 7 corresponds to the M33 planetary nebulae (PNe; Magrini et al. 2010), which are believed to be disk tracers with ages as old as 10 Gyr (Maraston 2005). Their abundances have been converted from $12 + \log (\text{O}/\text{H})$ to $[\text{Fe}/\text{H}]$ using the relation between $[\alpha/\text{Fe}]$ and $[\text{Fe}/\text{H}]$ from Barker & Sarajedini (2008) for M33 and assuming that $[\alpha/\text{Fe}] \approx [\text{O}/\text{Fe}]$. Also plotted in Figure 7 are representatives of the M33 halo population – nine halo globular clusters (open triangles) from Sarajedini et al. (2000) and the RRL variables from Sarajedini et al. (2006, open squares) and the present study (filled squares). The furthest M33 globular cluster (EC-1) is also plotted (Stonkute et al. 2008). We note that this is a modified version of Figure 20 in the work of Barker et al. (2007).

Figure 7 suggests that the metal abundance of the M33 disk decreases with increasing galactocentric distance. In contrast, the halo populations show no trend of metal abundance with radial position reminiscent of the halo globular cluster population in the Milky Way beyond 8 kpc from the Galactic center (Zinn 1985). This represents another piece of evidence supporting the assertion that the majority of the M33 RR Lyraes are members of its halo rather than its disk.

4. Summary and Conclusions

Studies of RR Lyrae variables in M31 and M33 are still in their infancy but there are a few points we can make with relative certainty. First, both galaxies do indeed harbor RR Lyrae variables in their halos, which suggests that, similar to the Milky Way, there is an old component ($\gtrsim 10$ Gyr) to the halos of M31 and M33. These variables have pulsational properties that are consistent with those in Oosterhoff I Galactic globular clusters. Furthermore, their mean metallicity of the RR Lyraes in each galaxy is consistent with that of its halo globular clusters. Much more work is left to be done. For example, wide-field time-domain surveys of M31 and M33 will better reveal the spatial distribution of their RR Lyraes. The capabilities of 30m telescopes will likely allow us to obtain kinematic and abundance information for the RR Lyraes in M31 and M33. We can then study the detailed properties of the earliest epochs of star formation in these galaxies. This has implications for how spiral galaxies fit into the Λ CDM paradigm for structure formation in the early universe.

The author gratefully acknowledges the work of a number of close collaborators that have contributed results to this review, especially Soung-Chul Yang, whose doctoral dissertation at the University of Florida is the source of much of the M33 RR Lyrae work. The template-fitting code we use originated with Andy Layden and has been integrated into our FITLC software by University of Florida graduate student Conor Mancone. Much of this work has been supported by NASA through grants from the Space Telescope Science Institute which is operated by the Association of Universities for Research in Astronomy, Incorporated, under NASA contract NAS5-26555.

References

- Alcock, C. et al. 2000, *AJ*, 119, 2194
 Barker, M. & Sarajedini, A. 2008, *MNRAS*, 390, 863
 Barker, M. K. et al. 2007, *AJ*, 133, 1138,
 Bono, G., Caputo, F., & Di Criscienzo, M. 2007, *A&A*, 476, 779
 Brown, T. M., Ferguson, H. C., Smith, E., Kimble, R. A., Sweigart, A. V., Renzini, A., & Rich, R. M. 2004, *AJ*, 127, 2738
 Chaboyer, B. 1999, in *Post-Hipparcos Cosmic Candles*, *ASSL*, Vol. 237, edited by A. Heck and F. Caputo (Dordrecht: Kluwer Academic Publishers) p.111
 Clement, C. M. & Rowe, J. 2000, *AJ*, 120, 2579
 Dolphin, A. E., Saha, A., Olszewski, E. W., Thim, F., Skillman, E. D., Gallagher, J. S. & Hoessel, J. 2004, *AJ*, 127, 875
 Dotter, A., Sarajedini, A., Anderson, J., Aparicio, A., Bedin, L. R. Chaboyer, B., Majewski, S., Marn-Franch, A., Milone, A., Paust, N., Piotto, G., Reid, I. N., Rosenberg, A., & Siegel, M. 2010, *ApJ*, 708, 698
 Durrell, P., Harris, W. E., & Pritchett, C. J. 2001, *AJ*, 121, 2557
 Galleti, S., Bellazzini, M., & Ferraro, F. R. 2004, *A&A*, 423, 925
 Gratton, R. G., Bragaglia, A., Carretta, E., Clementini, G., Desidera, S., Grundahl, F., & Lucatello, S., 2003, *A&A*, 408, 529
 Gratton, R. G., Bragaglia, A., Clementini, G., Carretta, E., Di Fabrizio, L., Maio, M., & Taribello, E. 2004, *A&A*, 421, 937
 Grebel, E. K., Gallagher, J. S. III, & Harbeck, D. 2003, *AJ*, 125, 1926
 Grillmair, C. et al. 1996, *AJ*, 112, 1975
 Guhathakurta, P. et al. 2005, arXiv preprint (astro-ph/0502366)
 Guldenschuh, K. et al. 2005, *PASP*, 117, 721
 Kalirai, J. S. et al. 2006, *ApJ*, 648, 389
 Kim, M. et al. 2002, *AJ*, 123, 244
 Koch, A., & Grebel, E. K. 2006, 131, 1405
 Koch, A., et al. 2008, *ApJ*, 689, 958
 Kunder, A., Chaboyer, B., & Layden, A. C. 2010, *AJ*, 139, 415
 Irwin, M. J., Ferguson, A. M. N., Ibata, R. A., Lewis, G. F., & Tanvir, N. R. 2005, *ApJ*, 628, L108
 Jeffery, E. J., Smith, E., Brown, T. M., Sweigart, A. V., Kalirai, J., Ferguson, H. C., Guhathakurta, P., Renzini, A., & Rich, R. M. 2011, *AJ*, in press (arXiv:1103.1400)
 Layden A. C., & Sarajedini, A. 2000, *AJ*, 119, 1760
 Magrini, L. et al. 2010, *A&A*, 512, A63
 Mancone, C. L. & Sarajedini, A. 2008, *AJ*, 136, 1913
 Maraston, C. 2005, *MNRAS*, 362, 799
 Martin, N. F. et al. 2006, *MNRAS*, 371, 1983
 Meylan, G. Sarajedini, A., Jablonka, P., Djorgovski, S. G., Bridges, T., & Rich, R. M. 2001, *AJ*, 122, 830
 Mould, J. & Kristian, J. 1986, *ApJ*, 305, 591
 Navarro, J. F., Frenk, C. S., & White, S. D. M. 1997, *ApJ*, 490, 493
 Oosterhoff, P. T. 1939, *The Observatory*, 62, 104
 Pritchett, C. J. 1988, in *The Extragalactic Distance Scale*, *ASP Conf. Ser.* (ASP: San Francisco) p. 59
 Pritchett, C. J. & van den Bergh, S. 1987, *ApJ*, 316, 517
 San Roman, I., Sarajedini, A., Garnett, D. R., & Holtzman, J. A. 2009, *ApJ*, 699, 839

- Sarajedini, A., & Jablonka, P. 2005, AJ, 130, 1627
Sarajedini, A., Geisler, D., Schommer, R. & Harding, P. 2000, AJ, 120, 2437
Sarajedini, A., Barker, M. K., Geisler, D., Harding, P., & Schommer, R. 2006, AJ, 132, 1361
Sarajedini, A., Mancone, C., Lauer, T. R., Dressler, A., Freedman, W., Trager, S. C. Grillmair, C., & Mighell, K. J. 2009, AJ, 138, 184
Smith, H. 1995, in RR Lyrae Stars, Cambridge Astrophysics Series, (Cambridge University Press: Cambridge) p. 14
Stonkute, R. et al. 2008, AJ, 135, 1482
Sturch, C. 1966, ApJ, 143, 774
Williams, B. F., Dalcanton, J. J., Dolphin, A. E., Holtzman, J., & Sarajedini, A. 2009, ApJ, 695, L15
Yang, S. -C., Sarajedini, A., Holtzman, J. A., & Garnett, D. R. 2010, ApJ, 724, 799
Zinn, R. J. 1985, ApJ, 293, 424